PHYSICAL REVIEW E VOLUME 53, NUMBER 3 MARCH 1996

Reaction-diffusion model for the hydration and setting of cement

F. Tzschichholz, H.J. Herrmann, and H. Zanni
Laboratoire de Physique et Mécanique des Milieux Hétérogènes, CNRS URA 857, École Supérieure de Physique et de Chimie Industrielle de la Ville de Paris, 10 rue Vauquelin, 75231 Paris Cedex 05, France

(Received 4 August 1995)

We propose a heterogeneous reaction-diffusion model for the hydration and setting of cement. The model is based on diffusional ion transport and on cement-specific chemical dissolution–precipitation reactions under spatial heterogeneous solid-liquid conditions. We simulate the spatial and temporal evolution of precipitated microstructures starting from initial random configurations of anhydrous cement particles. Though the simulations have been performed for two dimensional systems, we are able to reproduce qualitatively basic features of the cement hydration problem. The proposed model is also applicable to general water-mineral systems.

PACS number(s): 82.20.Wt, 61.43.–j, 81.05.Rm, 81.30.Mh

I. INTRODUCTION

In the present paper we propose a heterogeneous reaction-diffusion model for the hydration and setting of cement. The proposed model is based on the experimental observation that cement hydration can be described by a dissolution-precipitation mechanism [1–5].

The elementary aspects of the cement hydration-setting process on a mesoscopic length scale can be characterized as follows. At the initial stage cement particles or powder (in our case tricalcium silicate, Ca_3SiO_5) are mixed well with the solvent (water). Rapidly after mixing the *dissolution*, the reaction of the cement particles starts. Its principal reaction products are ions that are mobile and may *diffuse* into the bulk of the solvent (in our case Ca^{2+} , OH^-, and $H_2SiO_4^{2-}$ ions). At this stage the ion concentrations in the bulk of the solvent are very low and, as a consequence, one finds strong ion fluxes from the dissolution front away into the solvent. However, for a given temperature and pressure the ion concentrations cannot take arbitrary high values. Rather, the ion concentrations are bounded by finite solubility products above which solid phases start to *precipitate* from the solution. There are two associated precipitation reactions: (a) the precipitation of calcium hydro-silicate, sometimes referred to as "cement gel" [$\equiv(CaO)_{1.5}\,(SiO_2)\,(H_2O)_{2.5}$] and (b) the precipitation of calcium hydroxide or "Portlandite" [$\equiv Ca(OH)_2$] [3]. While the growth of the cement gel is the basis for the whole cement binding process, the growth of Portlandite mainly happens in order to compensate for the accumulation of Ca^{2+} and OH^- ions in solution (see below).

The process of cement dissolution, ion transport, and cement gel–Portlandite precipitation is usually referred to as "cement hydration." This process is to a high extent heterogeneous in the sense that starting from initially random cement particle positions, dissolution and precipitation reactions change the physical (boundary) conditions for the ion transports themselves. This is due to the fact that the diffusion within the solid phases can be neglected relative to the solvent one.

Coupled chemical dissolution-precipitation reactions are well known for a long time in geology and geochemistry. As such kinds of processes are fundamental for water-mineral systems, some effort has been undertaken to modelize such systems [6,7]. The approaches differ methodologically and focus on different physical and chemical aspects. Reference [6] considers the ion transport problem for a single, solubility controlled, dissolution-precipitation reaction employing a one dimensional cellular automaton approach. A chemically more detailed approach of water-mineral interactions includes considerations on the influence of nucleation, electro chemistry, and temperature on chemical reaction rates, however, without considering a transport equation [7].

Recently, a relatively simple stochastic cellular automaton model for cement hydration-setting has been proposed [8]. Therein it has been tacitly assumed that ion transport is not relevant for the hydration process above a certain mesoscopic length scale ("pixel size"). Furthermore, in this model hydrate "pixels" perform a random walk until they touch another solid "pixel," where they then stick [8,9]. We position our deterministic model into the "opposite" direction: mass transport happens due to diffusion of ions, and the hydrates are regarded as immobile.

In Sec. II we give a detailed description of the employed model. We consider heterogeneity aspects in Sec. II A, chemical aspects in Sec. II B, and transport aspects in Sec. II C. Section III contains first results. We present some images of calculated cement microstructures, which comprehensively demonstrate basic features and capabilities of the present approach. We consider parametric plots for the mean ion concentrations, known in cement literature as the "kinetic path approach," and compare our findings with experimental results [10]. Following this we investigate the variation of the maximum average silica concentration in solution for various chemical reaction rate constants. Finally we present curves for the hydration advancement in time for two different sets of reaction rate constants. In Sec. IV we summarize and give some ideas about future work.

1063-651X/96/53(3)/2629(9)/$10.00

II. THE MODEL

In the following we describe the proposed reaction diffusion model for the hydration and setting of cement in more detail. We will first discuss how to quantitatively describe the heterogeneities and outline some general features of the employed model. Following this we will summarize the dissolution-precipitation reactions and the employed reaction rate laws. Finally some physical aspects of the ion transport in the solvent are discussed. The latter one represents the *physical coupling* between the dissolution and precipitation reactions.

A. Heterogeneity aspects

We consider a discrete reaction-diffusion model in space and time. The physicochemical system can be regarded as being composed of "sufficient" small volume elements $V = \Delta x^3$ with Δx typically between 10^{-6} and 10^{-4} m. The initial configuration is determined from a digitized micrograph image as follows: the micrograph is immediately taken after mixing at time t_0, one can assume to find only the solid phase Ca_3SiO_5 and water (aq). By measuring the occupied volumes $V_i^{(\alpha)}$ of the phase α, $(\alpha = aq, Ca_3SiO_5)$, in each cell i using an image processing system, one determines the initial distribution of mole numbers $n_i^{(\alpha)}(t_0)$ according to $n_i^{(\alpha)}(t_0) = V_i^{(\alpha)}(t_0)/v^{(\alpha)}$. The $v^{(\alpha)}$ are known molecular volumes for room temperature; see Table I. In general, such a micrograph shows cement particles of different sizes immersed in water. Because each cell volume is completely filled with solid and solvent phases, one can calculate the solvent volume of cell i *at any time step* from the corresponding solid volume(s),

$$V_i^{(aq)}(t) = V - \sum_{\alpha \neq aq} n_i^{(\alpha)}(t) v^{(\alpha)}. \tag{2.1}$$

This is a useful equation, because ion concentrations are mostly calculated with respect to the actual solvent volume $V_i^{(aq)}(t)$. The physical constraints of Eq. (2.1) are that the chemical reactions must be *sufficiently slow* in comparison to the solvent flow. Furthermore, it is tacitly assumed that the whole system is connected to an external water reservoir in such a way that the solid phases do not hinder the flow.

In a given volume element the dissolution-precipitation reactions will, in general, not instantaneously go to completion. The solvent volume in each cell will rather increase or decrease continuously, defining a solvent distribution field,

$$\varepsilon_i^{(aq)}(t) = V_i^{(aq)}(t)/V. \tag{2.2}$$

The solid phase volume fractions $\varepsilon_i^{(\alpha)}(t)$ are defined analogously. The initial water to cement weight ratio w/c can be expressed through the initial average cement volume fraction $\langle \varepsilon^{(C_3S)}(t_0) \rangle$,

$$\frac{w}{c} = \frac{1 - \langle \varepsilon^{(C_3S)}(t_0) \rangle}{3.15 \, \langle \varepsilon^{(C_3S)}(t_0) \rangle}, \tag{2.3}$$

where the number 3.15 is the relative weight as calculated from Table I. We believe in fact that the time dependent volume fractions $\varepsilon_i^{(\alpha)}(t)$, reflecting the actual solvent-solid distribution in the system, are sufficient to characterize most of the aspects of the hydration process on a macroscopic length scale. Though we do not have information about these distributions on a length scale smaller than Δx we will assume that the reactants are homogeneously distributed in each volume element. The volume fractions may then be interpreted as probabilities to find at a random position within cell i the reactant α.

B. Chemical aspects

In the following we will summarize the considered dissolution-precipitation reactions and the employed re-

TABLE I. Stoichiometric numbers $\nu_1^{(\alpha)}$, $\nu_2^{(\alpha)}$, and $\nu_3^{(\alpha)}$ of the chemical reactions Eqs. (2.4), (2.6), and (2.8), respectively. The last three colums give the molecular volumes, the diffusion constants, and the solubilities at room temperature and normal pressure.

Species α	Stoichiometric numbers $\nu_1^{(\alpha)}$	$\nu_2^{(\alpha)}$	$\nu_3^{(\alpha)}$	Molecular volume (10^{-3} liter/mol)	Diffusion constant (10^{-10} m^2/s)	Solubility (10^{-3} mol/liter)
H_2O	−3	−1	0	18.01	0	—
Ca_3SiO_5	−1	0	0	73.1[a]	0	∞[b]
$(CaO)_{1.5}(SiO_2)(H_2O)_{2.5}$	0	1	0	80.40[c]	0	2.4[d]
$Ca(OH)_2$	0	0	1	33.07[e]	0	20.2[e]
Ca^{2+}	3	−3/2	−1	—	7.9[f]	—
OH^-	4	−1	−2	—	53.0[f]	—
$H_2SiO_4^{2-}$	1	−1	0	—	5.0[b]	—

[a] Reference [1], p. 15.

[b] Measured values are not known to us.

[c] Reference [1], p. 152. We assume for the calculations a density of 2.35 g/cm^{-3}.

[d] We have calculated this value from the supersaturation concentrations of calcium and silicate ions, as reported in Ref. [3].

[e] Reference [1], p. 125.

[f] Reference [11], p. 839.

action rate laws. During the course of the simulation it may happen that the reaction flux, as calculated from the kinetic equations, does exceed the available amounts of chemical reactants in a given cell. We therefore check at each time step and for each chemical reaction if there exists a limiting reactant. If this happens, we define the reaction flux through the amount of the available limiting reactant.

1. Ca_3SiO_5 dissolution

The Ca_3SiO_5 dissolution reaction is a spontaneous and exothermic *surface reaction* which happens at the Ca_3SiO_5-solvent interface(s) [3]. It can be considered as irreversible,

$$Ca_3SiO_{5(s)} + 3H_2O_{(\ell)} \xrightarrow{k_1} 3Ca^{2+}_{(aq)} + 4OH^-_{(aq)} + H_2SiO^{2-}_{4(aq)}. \tag{2.4}$$

Here k_1 denotes an appropriate surface reaction constant in units of $\mathrm{mol\,m^{-2}\,s^{-1}}$.

Chemical reactions must be considered as local, i.e., each volume element is acting as a small and independent chemical reactor as long as no transport occurs. However, for a pronounced dissolution reaction in a given cell one has also to consider the possible reaction amounts originating from the interfaces with its neighboring cells. This can be done by allowing cement dissolution in cell i through a fraction γ of the solvent of the neighboring cells j,

$$\nu_1^{(\alpha)}\, d\xi_{i,1}(t) = \nu_1^{(\alpha)}\, k_1\, \Delta t\, \Delta x^2 \left[p_{ii} + \gamma \sum_{j=nn(i)} (p_{ij} - p_{ii}) \right]. \tag{2.5}$$

Here $\nu_1^{(\alpha)}$ denote the stoichiometric numbers of species α in reaction (2.4); see Table I. The changes in mole numbers of species α in cell i in a time interval Δt due to this reaction are denoted by $\nu_1^{(\alpha)}\, d\xi_{i,1}(t)$. The sum on the right-hand side has to be taken over all next nearest neighboring cells of cell i, as indicated by $j = nn(i)$. The first term $p_{ii} = \varepsilon_i^{(Ca_3SiO_5)} \varepsilon_i^{(aq)}$ in Eq. (2.5) describes the dissolution within cell i ($\gamma = 0$) due to a "typical" reaction interface. It can be understood as a probability to find the two reactants, Ca_3SiO_5 and water, in contact at an arbitrary chosen point within cell i. The "chemically active interface" between cell i and j is given by $p_{ij}\Delta x^2 = \Delta x^2 \varepsilon_i^{(Ca_3SiO_5)} \varepsilon_j^{(aq)}$. The constant γ controls the degree of dissolution due to this interface(s). We have used a value $\gamma = 1/8$ in our simulations, yielding comparable reaction rates from inner and outer cell surfaces. The determination of the reaction interfaces in terms of cement and water volume fractions is similar to the degree of surface coverage used in Langmuir absorption theory [11]. However, the absorption of water on the cement's surface and the desorption of ions from this surface are not necessarily the rate determining steps. In fact, the dissolution reaction (2.4) involves various physical and chemical subprocesses [5], which will not be considered here.

2. Cement gel dissolution-precipitation

The precipitation of $(CaO)_{1.5}(SiO_2)(H_2O)_{2.5}$ is an endothermic reaction that can be considered as reversible [3],

$$(CaO)_{1.5}(SiO_2)(H_2O)_{25} \overset{k_2}{\rightleftharpoons} H_2SiO^{2-}_{4(aq)} + 1.5Ca^{2+}_{(aq)} + OH^-_{(aq)} + H_2O_{(\ell)}, \tag{2.6}$$

having a forward (dissolution) rate constant k_2 (in units of $\mathrm{mol\,m^{-2}\,s^{-1}}$).

We note that the cement gel precipitation, i.e., the backward reaction in Eq. (2.6) is the main reaction in this balance equation. The reactants and products are considered to have a fixed stoichiometry. However, it is known from experimental data that the stoichiometry of $(CaO)_x(SiO_2)_y(H_2O)_z$ can be rather variable ("solid solution") [2]. We will not include these complications into the model. Instead we consider a fixed and typical calcium-silica ratio equal to 1.5 [2].

In equilibrium the $(CaO)_{1.5}(SiO_2)(H_2O)_{2.5}$ dissolution-precipitation reactions are controlled by an empirical value of solubility, giving the maximum amount of solid one can dissolve in aqueous solution at a given temperature (room temperature) and pressure (normal pressure). Employing this empirical solubility constant one can directly determine the equilibrium solubility product, $S_2^{equi} = S_{2i}|^{equi} = [Ca^{2+}]_i^{1.5}[OH^-]_i[H_2SiO_4^{2-}]_i|^{equi} \approx 1.2 \times 10^{-9}\,\mathrm{mol^{3.5}\,liter^{-3.5}}$; cf. Table I. The square brackets denote the ion concentrations with respect to the available solvent, i.e., $[Ca^{2+}]_i = n_i^{(Ca^{2+})}/V_i^{(aq)}$, etc. When in a given cell the ion product is larger than the solubility product, locally precipitation happens. If it is lower, $(CaO)_{1.5}(SiO_2)(H_2O)_{2.5}$ becomes dissolved. The cement gel dissolution is only marginal and for this reason we will employ for the rate of dissolution a simpler expression than for the Ca_3SiO_5 dissolution reaction.

We assume that the dissolution reaction in cell i is proportional to the typical reaction interface $\Delta x^2 \varepsilon_i^{(aq)}$ with the dissolution constant k_2 as the constant of proportionality. The precipitation reaction is assumed to be proportional to the reaction interface and proportional to the ion product S_{2i}, as defined above. The rate constant of the precipitation reaction can be eliminated, by use of the equilibrium condition, $d\xi_{i,2} = 0$. We have employed the following rate equation,

$$\nu_2^{(\alpha)}\, d\xi_{i,2}(t) = \nu_2^{(\alpha)}\, k_2\, \Delta t\, \Delta x^2\, \varepsilon_i^{(aq)} \left(1 - \frac{S_{2i}}{S_2^{equi}} \right). \tag{2.7}$$

The stoichiometric numbers again are denoted by $\nu_2^{(\alpha)}$, see Table I, and the change in mole numbers of species α due to this reaction is $\nu_2^{(\alpha)}\, d\xi_{i,2}(t)$.

3. Ca(OH)$_2$ dissolution-precipitation

The precipitation of calcium hydroxide accompanies the cement gel precipitation. This is because the cement gel precipitation does not consume the ions in the same proportions as they are released due to Ca_3SiO_5 dissolution. The non-reacted Ca^{2+} and OH^- ions soon begin to accumulate in solution, until the solubility of $Ca(OH)_2$ is exceeded. However, the precipitation of $Ca(OH)_2$ and cement gel are, in general, not simultaneous because the corresponding solubilities are very different; cf. Table I. The dissolution-precipitation of $Ca(OH)_2$ can be considered as reversible,

$$[\mathrm{Ca(OH_2)}]_{(s)} \overset{k_3}{\rightleftharpoons} \mathrm{Ca}^{2+}_{(aq)} + 2\mathrm{OH}^{-}_{(aq)}, \tag{2.8}$$

having a dissolution constant k_3 $(\mathrm{mol\,m^{-2}\,s^{-1}})$.

The corresponding solubility product for $Ca(OH)_2$ is defined as $S_3^{equi} = S_{3i}|^{equi} = [\mathrm{Ca}^{2+}]_i[\mathrm{OH}^-]_i^2|^{equi} \approx 3.3 \times 10^{-6}\,\mathrm{mol^3\,liter^{-3}}$, which is about three orders of magnitude larger than S_2^{equi}; see Table I,

$$\nu_3^{(\alpha)}\, d\xi_{i,3}(t) = \nu_3^{(\alpha)}\, k_3\, \Delta t\, \Delta x^2\, \varepsilon_i^{(aq)} \left(1 - \frac{S_{3i}}{S_3^{equi}}\right). \tag{2.9}$$

In all other respects the $Ca(OH)_2$ reaction is treated analogously to the cement gel dissolution-precipitation reaction.

4. Chemical shrinkage

One can write down from Eqs. (2.4), (2.6), and (2.8) the net reaction for the cement hydration process,

$$(\mathrm{Ca_3SiO_5})_{(s)} + 4\mathrm{H_2O}_{(\ell)} \rightharpoonup \mathrm{CaO_{1.5}(SiO_2)(H_2O)_{2.5(s)}} + 1.5[\mathrm{Ca(OH)_2}]_{(s)}. \tag{2.10}$$

Calculating for the above equation the occupied volumes for one mole, one finds for the left-hand side approximately 144 cm^3 and for the hydrate products 130 cm^3, see Table I. Hence, the reaction products occupy a volume around 10% smaller than the reactants (including solvent). This effect, which is typical for hydraulic binders, is termed "chemical shrinkage" or Le Chatelier effect. Wherever topologically possible water flow will try to compensate for the loss of volume. However, in the course of an experimental cement setting and hardening (rigidification) process available solvent flow paths may vanish and volume loss becomes partially compensated building up mechanical deformations (stresses) within the solid phase agglomerate. In turn these stresses influence the reaction rates (which in general are pressure dependent) in a complex manner [4]. The appearance of voids (pores) on the submicron scale is experimentally also well established [1].

We will not modelize such complex problems as mechanical stresses, solvent cavitation, and solvent flow due to chemical shrinkage in our present approach. Instead we will assume throughout all calculations that the solvent is able to balance the chemical shrinkage for all time steps and for all volume elements according to Eq. (2.1). This assumption is equivalent to the introduction of local source terms for water, i.e., the hydrating system is connected to an external water reservoir in an appropriate way.

We would like to point out that Eq. (2.10) is an overall reaction that per definition only holds for an isolated system. On the other hand, one cannot treat the volume elements as chemically isolated, simply because of the ion fluxes going through the elements. This and the different values for the cement gel and $Ca(OH)_2$ solubilities imply in general locally noncongruent precipitation reactions. As a consequence one cannot simply "replace" one dissolved unit volume of Ca_3SiO_5 by 1.7 unit volumes of cement gel and 0.6 unit volumes of $Ca(OH)_2$, as has been proposed in [8].

C. Transport aspects

It is known from experiments that ion transport due to diffusion is fundamental in cement chemistry, because of very strong ion concentration gradients close to the dissolving Ca_3SiO_3 solvent interface(s). In general one should consider the convective diffusion equation; however, this would imply solving the hydrodynamic equations. In the present paper we consider the usual diffusion equation with local, appropriately defined transport coefficients. It is, in the context of the investigated problem, useful to consider only the ion diffusion within the solvent. For convenience we document in Table I the diffusion constants $D^{(\alpha)}$ as calculated from the electric mobilities at room temperature and normal pressure for infinite dilution. The solids' and the solvent's diffusion constants are set to zero [12]. This allows a relatively compact notation for the equations of continuity,

$$\Delta n_i^{(\alpha)} = \frac{\Delta t}{\Delta x^2} V \sum_{j=nn(i)} \left(D_{ij}^{(\alpha)} c_j^{(\alpha)} - D_{ij}^{(\alpha)} c_i^{(\alpha)}\right) + \sum_{k=1}^{3} \nu_k^{(\alpha)}\, d\xi_{i,k}. \tag{2.11}$$

The second term on the right-hand side of Eq. (2.11) represents the already known source term due to the chemical reactions Eqs. (2.5), (2.7), and (2.9). The $D_{ij}^{(\alpha)}$ are the transport coefficients, which depend on the solvent volume fractions (porosities) of the cells involved in the diffusion process, $D_{ij}^{(\alpha)} = D^{(\alpha)}\varepsilon_i^{(aq)}\varepsilon_j^{(aq)}$. The ion concentrations are taken with respect to the actual solvent volume, i.e., $c_i^{(\alpha)} = n_i^{(\alpha)}/V_i^{(aq)}$. We have employed periodic boundary conditions in all calculations.

The general formulation of the ion transport problem in cement chemistry involves various subproblems which we will not consider at this stage of modelization, as there are the transports due to

1. Heat conductance

The cement dissolution reaction is strongly exothermic. Analogous to the concentration gradients one finds near the various dissolution fronts strong temperature gradients, leading to nonisothermal solvent flow fields, with its complications. The heat redistribution is probably also of direct importance for the dissolution-precipitation reactions, because their reaction constants, as well as the corresponding solubility products, usually depend very sensitively on the temperature. We will neglect this possible effects in our approach assuming an overall constant room temperature, $T_0 = 298$ K.

2. Electrostatic interactions

Because one is dealing with the transport of electrically charged particles, one must consider, in general, Poisson's equation for the electrostatic potential in order to determine the resulting ion mobilities due to their electric field. We will neglect in our simulations all electrostatic interactions. Furthermore, all chemical rate calculations are done in terms of molar concentrations and not in terms of "chemical activities" (which is equivalent in the limit of infinite dilution). Hence we will treat the ions in solution as uncharged particles throughout all calculations.

3. Solvent flow

This is possibly of importance for the overall hydration process, because the solvent has to move during the dissolution-precipitation reactions accordingly, in order to compensate for the loss or gain of solid volume, creating advective ion fluxes. For an infinite, plane cement-water interface one might argue that the solvent flow is always perpendicular to the interface. Under these particular conditions it can be shown by scaling arguments that advective ion transport is unimportant relative to the diffusion transport, because of the relatively low molecular volume of cement; cf. Table I. However, in a finite heterogeneous system solvent flows tangential with respect to the interfaces are also expected, and the argument given above is limited. In principle one has to consider the equations of hydrodynamics for this purpose. However, this moving boundary problem is complex and we will not consider it in this form here. Instead we will determine the spatial and temporal solvent distribution $V_i^{(aq)}(t)$ according to Eq. (2.1).

III. RESULTS

From a general point of view cement hydration can be regarded as a heterogeneous (nonequilibrium) solid phase transformation forming, from an anhydrous solid phase, two hydrated solid phases [13]. In contrast to known solid-solid phase transformations, for example, in metallic alloys, cement hydration is based strongly on the presence of a solvent phase (mostly water). The solvent controls the transformation in a twofold sense: it is directly part of the chemical reactions and, on the other hand, it controls the ion transport to a very large extent.

The complexity of the problem and the features of the present approach are most conveniently illustrated by Fig. 1. Therein we show the solid volume fractions of anhydrous cement, $\varepsilon^{\mathrm{Ca_3SiO_5}}$ (left-hand side), and of hydrated cement, $\varepsilon^{(\text{cement gel})}$ (right-hand side), for three different hydration times (a) $t = 1500$ s, (b) $t = 2500$ s, and (c) $t = 5000$ s. The occupied volume fractions are color coded ranging from blue (0–20%), cyan (20–40%), green (40–60%) over yellow-orange (60–80%) to red (80–100%). The calculated micrographs Figs. 1(a)–1(c) show, as expected, spatially inhomogeneous nucleation and growth of cement gel hydrate. The hydrate precipitation and the associated growth of hydrate surface layers surrounding dissolving cement particles is relatively slow. However, in Fig. 1(b) one especially observes that the rate of cement gel precipitation is spatially strongly varying (notice the red and cyan spots in the right image). This reflects the spatial fluctuations in chemical reactivities (local $\mathrm{Ca_3SiO_5}$ surface to volume ratio), i.e., the reactivity of a "fjord" is higher than that of a big "lake". With support from experimental observations, it has been argued that cement particle surfaces close to each other may indeed act as very strong inhomogeneities leading to localized cement gel nucleation forming "bridges" between adjacent particles [14]. Our micrographs confirm this picture. We note that the proposed model does not include any (auto)catalytic effect of cement gel or $\mathrm{Ca(OH)_2}$ on the hydrate growth, yet, compare Eq. (2.7). This point is intensively studied at the moment.

As the hydrate precipitation-dissolution reaction rates depend on the local supersaturation values, the interesting question arises how global characteristic points of the cement hydration kinetics can be defined. In a recent experimental work it has been proposed to characterize different kinetic regimes occurring during the $\mathrm{CaSiO_5}$ hydration by means of parametric plots of "typical" calcium versus silicate concentrations as estimated from calorimetric or conductimetric measurements ("kinetic path approach") [10]. The experiments have been conducted employing stirred diluted $\mathrm{Ca_3SiO_5}$ suspensions having a water to cement weight ratio between 10 and 50; cf. Eq. (2.3). However, to obtain typical quantities of such diluted suspensions employing numerical simulations one would have to consider very large systems. Instead we will compare the experimental suspension data with numerical cement paste data having a water to cement weight ratio close to the practically important value 0.5.

For convenience we reproduce in Fig. 2 some of the experimental data ($\diamond$) of Ref. [10]. Initially one finds an "inductive" cement dissolution period (period AB in Fig. 2). During this period the bulk solution is undersaturated everywhere with respect to cement gel and $\mathrm{Ca(OH)_2}$ the concentration gradients close to the cement particles are very high, and ions rapidly distribute into the bulk solvent. We have observed in our simulations that cement gel is already formed during the "induction" period, however, to a very low extent. Because of the initially very high concentration gradients the ion products exceed the cement gel solubility only in a very thin layer surrounding the cement particles. As the ions cu-

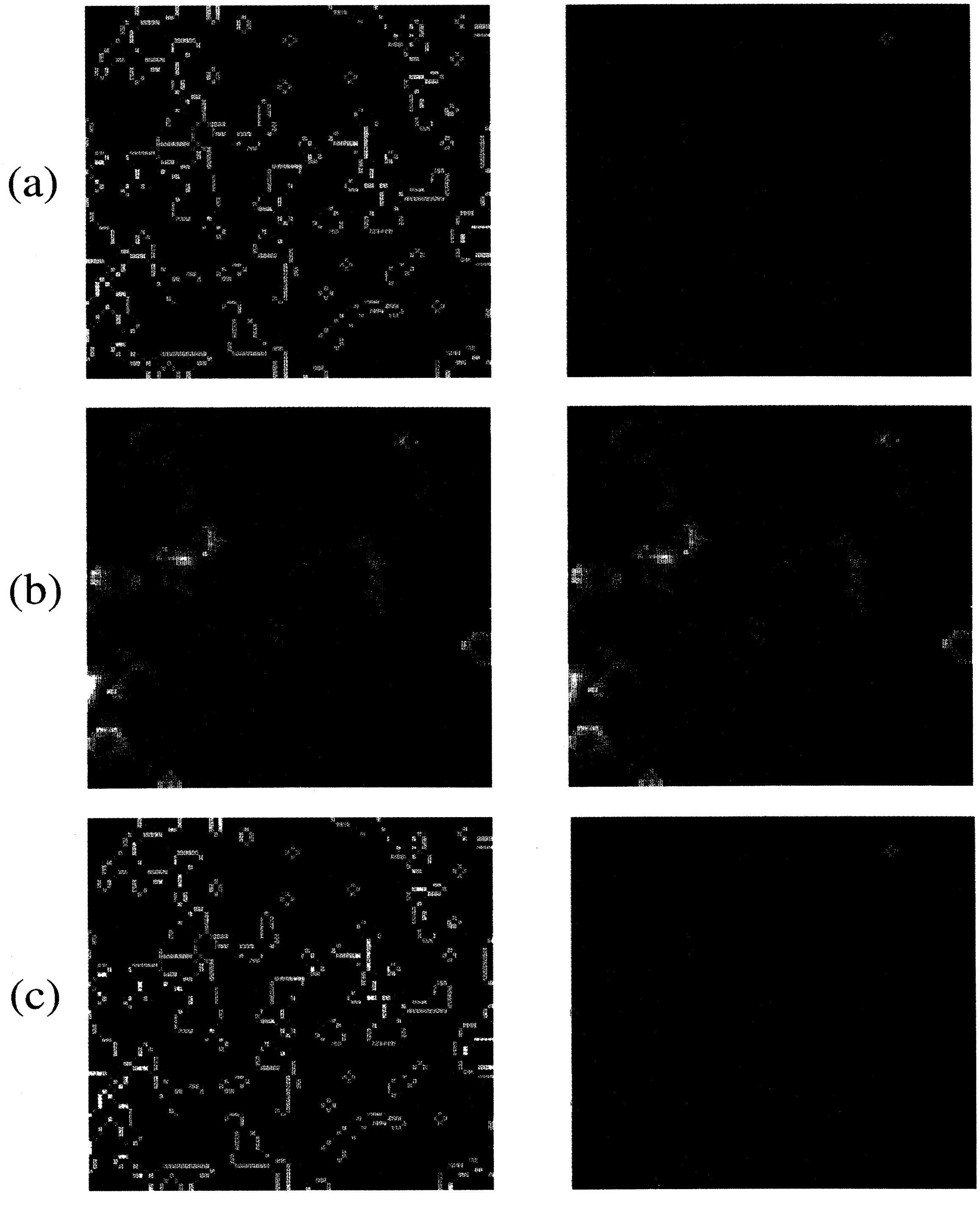

FIG. 1. Above figures show numerically calculated cement microstructures after (a) $t = 1500$ s, (b) $t = 2500$ s and (c) $t = 5000$ s. Images on the left-hand side show the unhydrated cement phase Ca_3SiO_5 while those on the right-hand side represent the hydrated, precipitated cement (cement gel). The colors indicate the local solid volume fractions, i.e., blue (0–20%), cyan (20–40%), green (40–60%), yellow-orange (60–80%), and red (80–100%). The initial water to cement ratio is about 0.4, the reaction rate constants are $k_1 = 10^{-3}$, $k_2 = 10^{-12}$, and $k_3 = 10^{-10}$ (in units of $\mathrm{mol\,m^{-2}\,s^{-1}}$). The employed cell size is $\Delta x = 10^{-4}\,\mathrm{m}$, the linear system size $L = 100\Delta x$, and the linear cement particle size $\ell = 5\Delta x$. The time step is 0.01 s. All other parameters are the same as in Table I.

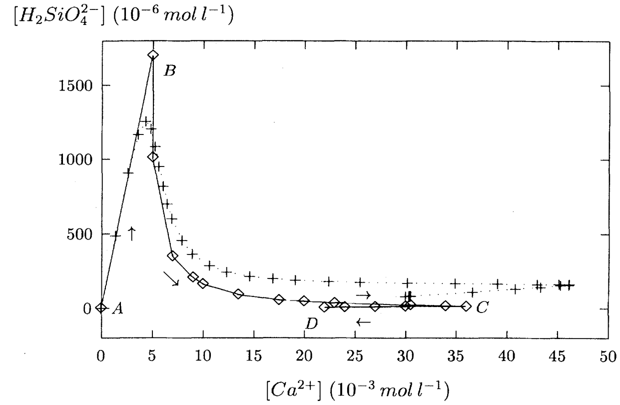

FIG. 2. Parametric plot of the evolution of silica versus calcium concentration (“kinetic path approach”); (◇) experimental results after Ref. [10], (+) numerical results. The employed reaction rate constants are $k_1 = 5 \times 10^{-5}$, $k_2 = 10^{-6}$, and $k_3 = 10^{-8}$ (in units of $\mathrm{mol\,m^{-2}\,s^{-1}}$). The linear system size is $L = 50\Delta x$, the cell size $\Delta x = 10^{-4}\,\mathrm{m}$, and the linear cement particle size $\ell = 5\Delta x$. The employed time step is 0.1 s. Initial water to cement weight ratio 0.6. All other parameters are the same as in Table I.

mulate in solution the thickness of this precipitating layer increases due to the broadening of the ion distributions.

The precipitation counteracts the further increase in silica concentration both by chemical reaction and by decreasing the cement particles surface permeability. As a result the silica concentration passes through a maximum (point B in Fig. 2), which might be interpreted as a *global measure* for the onset of cement gel precipitation. During the period BC the silica concentration decreases, while the calcium and hydroxyl concentrations continue to increase as the cement gel precipitation consumes only a fraction of these ions; see Eqs. (2.4) and (2.6).

Typically after a couple of hours the solution becomes oversaturated with respect to calcium hydroxide $\mathrm{Ca(OH)_2}$ (point C in Fig. 2). Both hydrates precipitate very slowly (experimentally several weeks between points C and D), lowering both calcium and hydroxyl concentrations. Point D corresponds to the state after infinite hydration time terminating the shown curve. The progress in time is indicated by arrows. Our numerical results (+) are in reasonable agreement with the experimental data (◇). We have observed that calculated positions and values for point C depend (a) on the employed initial water to cement weight ratio and (b) on the three reaction rate constants k_1, k_2, and k_3 in a rather complex manner. Contrary to this point B is found to depend only slightly on the *relative* reaction rate constant k_1/k_2 over four orders of magnitude; see Fig. 3(a). A consequence of the much smaller solubility of cement gel as compared to the second hydrate $\mathrm{Ca(OH)_2}$ is that in the period AB only *two* chemical reactions are operative. Reaction Eq. (2.8) is inoperative. For k_1/k_2 ranging between 0.1 and 10 the maximum silica concentrations take constant values of about 1 mmol/liter, while for $k_1/k_2 = 10^3$ we find ≈ 3 mmol/liter. We have also performed simulations for similar k_1/k_2 values employing different *absolute* reaction rate constants; see Fig. 3(a). We find a relatively good data collapse over four orders of magnitude. This result is important insofar as the reaction rate constants have not been experimentally measured yet. In Fig. 3(b) we plot the momentaneous calcium concentration versus the silica concentration at point B for various reaction rate constants. The data are centered around a straight line of slope 1/3. A comparison of this result with the stoichiometric coefficients in Eq. (2.4) shows that the silica/calcium ratio of ions is determined by the dissolution reaction.

The characterization of the temporal advancement of the hydration process is an important problem. We show in Fig. 4 some preliminary results for the time dependence of the mean volume fraction $\langle \varepsilon^{(\mathrm{cement\ gel})} \rangle$ of the cementious hydrate cement gel. For “moderate” reac-

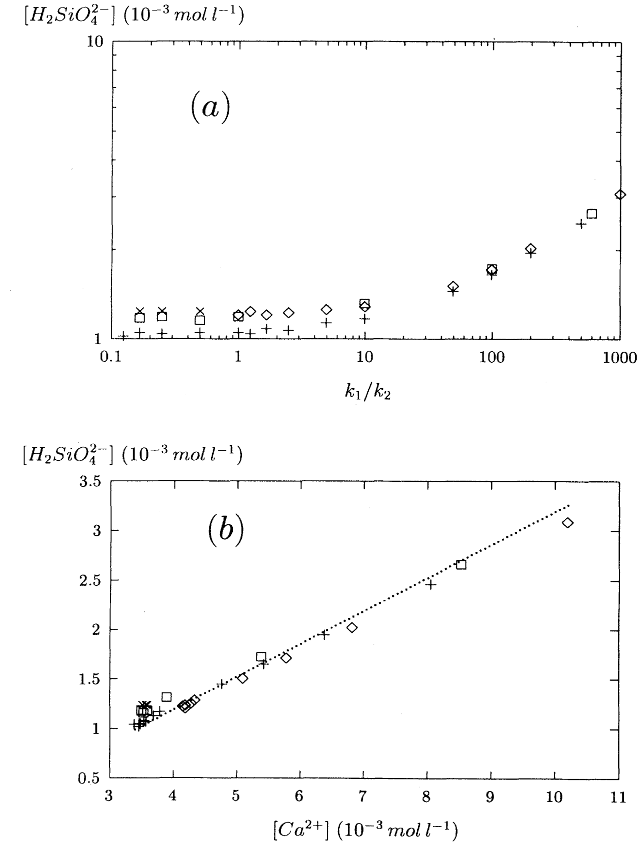

FIG. 3. Calculated silica ion concentration $[\mathrm{H_2SiO_4^{2-}}]$ at the onset of cement gel precipitation (corresponding to point B in Fig. 2): (a) double logarithmic plot versus the relative reaction rate constant k_1/k_2, (b) plot against the momentaneous $[\mathrm{Ca^{2+}}]$ ion concentration. Symbols: (◇) $k_1 = 10^{-4}\,\mathrm{mol\,m^{-2}\,s^{-1}}$, k_1/k_2 ranging between 1 and 1000; (+) $k_1 = 10^{-5}\,\mathrm{mol\,m^{-2}\,s^{-1}}$, k_1/k_2 ranging between 0.125 and 500; (□) $k_1 = 10^{-6}\,\mathrm{mol\,m^{-2}\,s^{-1}}$, k_1/k_2 ranging between 0.167 and 600; (×) $k_1 = 10^{-7}\,\mathrm{mol\,m^{-2}\,s^{-1}}$, k_1/k_2 ranging between 0.167 and 0.5. Each point corresponds to an average over 10 configurations having an initial water to cement weight ratio of about 0.5. All other parameters are the same as in Fig. 2.

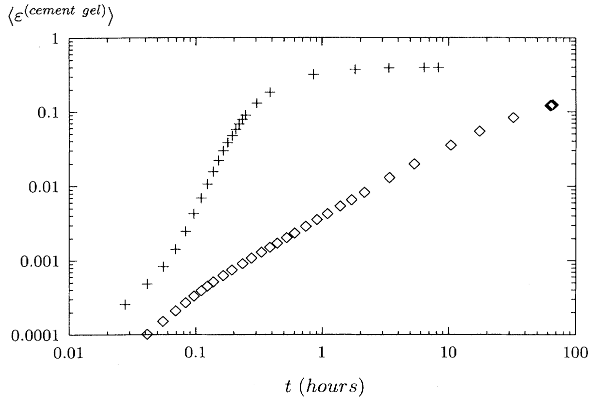

FIG. 4. Double logarithmic plot of the average cement gel volume fraction $\langle \varepsilon^{(\text{cement gel})} \rangle$ versus hydration time t for two sets of reaction rate constants: ($\diamond$) $k_1 = 5 \times 10^{-5}$, $k_2 = 10^{-6}$, and $k_3 = 10^{-8}$; (+) $k_1 = 10^{-2}$, $k_2 = 10^{-16}$, and $k_3 = 10^{-13}$; units in mol m^{-2} s^{-1}. All other parameters are the same as in Fig. 2.

tion constants ($\diamond$) the hydration is found to be relatively slow, i.e., after 70 h of hydration we find only 10% cement gel. This value is approximately two times lower than the experimental one observed by NMR measurements [15]. We note that both the hydration curve ($\diamond$) in Fig. 4 and the parametric curve (+) in Fig. 2 belong to the same simulation. Apparently the hydration advancement for "moderate" reaction rates is nearly constant in time; see curve ($\diamond$) in Fig. 4. For comparison we also show in Fig. 4 a hydration curve for "fast" hydration (+). After a few minutes of "induction" period the hydration rapidly accelerates and goes already after 1 h to completion (remaining Ca_3SiO_5 less than 1%). This process is much too fast and it leads to typical ion concentrations of mol/liter which are unrealistically high.

As long as the reaction rate constants have not been estimated from experiments yet one main difficulty in the modelization of cement hydration consists in finding appropriate values for the rate constants, *which do not contradict* experimental measurements of mean ion concentrations and hydration advancement. However, the experimental results belong to hydration in space, while our calculations correspond to two dimensional hydration. This point is currently being investigated.

IV. CONCLUSIONS

We have presented a general, heterogeneous reaction-diffusion model for solid phase transformation due to chemical dissolution-precipitation reactions. The model has focused on the important industrial problem of Portland cement hydration though it is more generally applicable to water-mineral systems.

We have tried to develop an "open" approach based on physical and chemical considerations (mainly the laws of mass conservation and mass action). The model includes in its present form on a coarse grained length and time scale the full spatial distribution of solid and liquid phases, the three main chemical dissolution-precipitation reactions, and the transport of ions due to diffusion. The proposed approach naturally allows the inclusion of a varity of more or less important phenomena depending on imposed conditions such as solvent flow effects, electrochemical effects, exothermic effects including heat conduction, pressure effects, inert filler effects, etc.

We have tried to incorporate a reasonable amount of specific information about the cement hydration into the investigated model, such as the stoichiometry and kinetics of Portland cement dissolution, the precipitation-dissolution of the main cementious hydrate (cement gel) and of Portlandite $Ca(OH)_2$, their approximate solubilities and molecular volumes, approximate values for the ion diffusivities in aqueous solution, and initial conditions for water immersed cement particles (sizes and spatial positions). The presented results demonstrate considerable richness and complexity of the cement hydration phenomenon close to controlled experimental situations.

We have presented some calculated cement microstructures as they evolve in time. Nucleation and growth of hydrates is found to be strongly heterogeneous in agreement with experimental observations. The problem of "autocatalytic" effects on the precipitation processes needs further investigation.

The presented parametric plots for the average concentrations of ions in solution are in qualitative agreement with recent indirect experimental observations made for stirred cement suspensions [10]. The calculated maximum silica concentrations and their corresponding calcium concentrations are in reasonable quantitative agreement with experimental values. For high dissolution and low precipitation rate constants we find unacceptable high ion concentrations of order mol/liter. One way to circumvent this problem would be the introduction of a *finite* solubility for Ca_3SiO_5 in Eq. (2.5); however, such a solubility constant has not been experimentally determined yet.

Furthermore we have investigated the variations of the maximum silica concentrations for various reaction rate constants. The concentrations are found to vary only slightly with the relative reaction rate constant k_1/k_2 over four orders of magnitude. It would be very interesting to see how the second characteristic hydration point (point C in Fig. 2) depends on the initial water to cement ratio and on the employed reaction rate constants.

Finally we presented results on overall hydration curves. These curves are not very realistic yet. It would be very helpful to have experimental order of magnitude estimates for the three (unknown) reaction rate constants. We are planning to conduct calculations in three dimensions with improved kinetic equations in a future work.

ACKNOWLEDGMENTS

We would like to acknowledge stimulating and interesting discussions with Ch. Vernet, H. Van Damme, S. Schwarzer, A. Nonat, and D. Damidot. F.T. would also like to acknowledge financial support from CNRS, from GDR project "Physique des Milieux Hétérogènes Complexes," and from Lafarge Coppee Recherche.

[1] H.F.W. Taylor, *Cement Chemistry* (Academic Press, London, 1990).

[2] P. Barret and D. Bertrandie, J. Chim. Phys. **83**, 765 (1986).

[3] D. Damidot and A. Nonat, in *Hydration and Setting of Cements*, edited by A. Nonat and J.C. Mutin (E&F Spon, London, 1992), p. 23.

[4] M. Michaux, E.B. Nelson, and B. Vidick, in *Well Cementing*, edited by E.B. Nelson (Schlumberger Educational Services, Housten, 1990), pp. 2-1.

[5] See, for example, C. Vernet, *Introduction à la Physicochimie du Ciment Portland. Deuxième Partie. Chimie de l'Hydratation* (Technodes S.A., Groupe Ciments Francais, Paris, 1992).

[6] T. Karapiperis (unpublished); T. Karapiperis and B. Blankleider, Physica D **78**, 30 (1994).

[7] B. Madé, A. Clément, and B. Fritz, Revue de l'Institut Francais du Petrole **49**, 6 (1994).

[8] D.P. Bentz and E.J. Garboczi, Cem. Concr. Res. **21**, 325 (1991); E.J. Garboczi and D.P. Bentz, J. Mater. Sci. **27**, 2083 (1992).

[9] D.P. Bentz, P.V. Coveney, E.J. Garboczi, M.F. Kleynl and P.E. Stutzman, Mode. Simul. Mater. Sci. Eng. **2**, 783 (1994).

[10] D. Damidot and A. Nonat, Adv. Cem. Res. **6** (21), 27 (1994); **6** (22), 83 (1994); D. Damidot, A. Nonat, P. Barret, D. Bertrandie, H. Zanni, and R. Rassem, *ibid.* **7** (25), 1 (1995).

[11] R.A. Alberty and R.J. Silbey, *Physical Chemistry* (Wiley & Sons, New York, 1992), p. 839.

[12] As aforementioned we determine the solvent volume and its mole numbers exclusively from Eq. (2.1). This assumption is reasonable as long as the number of solvated ions is much lower than the number of solvent molecules.

[13] It has been reported that under very particular experimental conditions (strongly diluted suspensions) the precipitation of calcium hydroxide becomes suppressed; see Ref. [14].

[14] A. Nonat, Mater. Struct. **27**, 187 (1994).

[15] C.M. Dobson, D.G.C. Goberdhan, J.D.F. Ramsay, and S.A. Rodger, J. Mater. Sci. **23**, 4108 (1988).

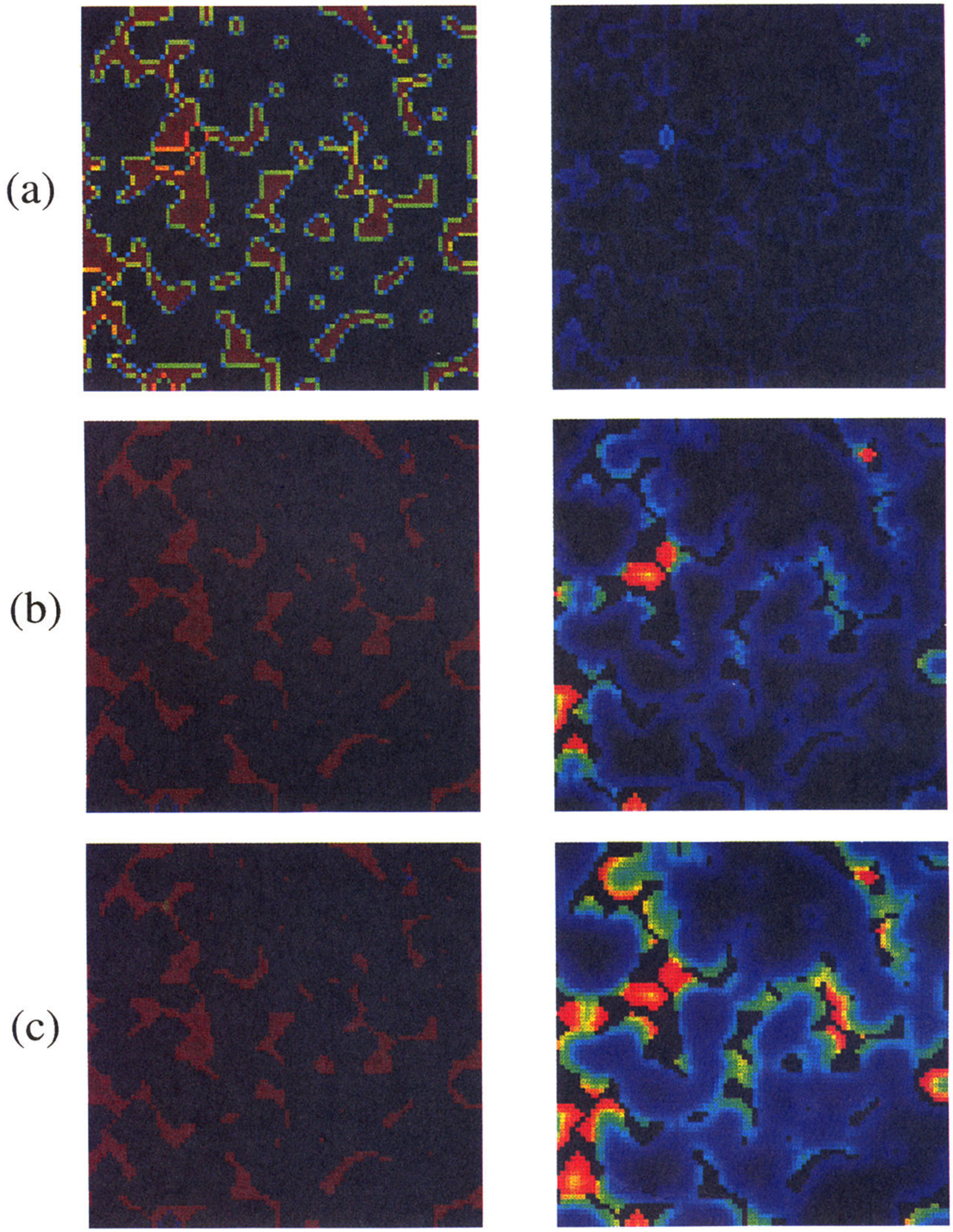

FIG. 1. Above figures show numerically calculated cement microstructures after (a) $t = 1500$ s, (b) $t = 2500$ s and (c) $t = 5000$ s. Images on the left-hand side show the unhydrated cement phase Ca_3SiO_5 while those on the right-hand side represent the hydrated, precipitated cement (cement gel). The colors indicate the local solid volume fractions, i.e., blue (0–20%), cyan (20–40%), green (40–60%), yellow-orange (60–80%), and red (80–100%). The initial water to cement ratio is about 0.4, the reaction rate constants are $k_1 = 10^{-3}$, $k_2 = 10^{-12}$, and $k_3 = 10^{-10}$ (in units of $\mathrm{mol\,m^{-2}\,s^{-1}}$). The employed cell size is $\Delta x = 10^{-4}\,\mathrm{m}$, the linear system size $L = 100\Delta x$, and the linear cement particle size $\ell = 5\Delta x$. The time step is 0.01 s. All other parameters are the same as in Table I.